Catastrophic Crystal Growth of Clathrate Hydrate with a Simulated Natural Gas System during a Pipeline Shut-In Condition

ARTICLE *in* CRYSTAL GROWTH & DESIGN · JANUARY 2015

Impact Factor: 4.89 · DOI: 10.1021/cg501626h

4 AUTHORS, INCLUDING:

Khalik M. Sabil

Heriot Watt Malaysia

47 PUBLICATIONS **189** CITATIONS

SEE PROFILE

Bhajan Lal

Universiti Teknologi PETRONAS

34 PUBLICATIONS **182** CITATIONS

SEE PROFILE

Paul Hammonds

Cairn India Ltd

12 PUBLICATIONS **20** CITATIONS

SEE PROFILE

CRYSTAL GROWTH & DESIGN

Article

pubs.acs.org/crystal

Catastrophic Crystal Growth of Clathrate Hydrate with a Simulated Natural Gas System during a Pipeline Shut-In Condition

Jega Divan Sundramoorthy,[†] Khalik M. Sabil,*[,#] Bhajan Lal,[§] and Paul Hammonds[‡]

[†]Baker Hughes (M) Sdn. Bhd, 207 Jalan Tun Razak, 50400 Kuala Lumpur, Federal Territory of Kuala Lumpur, Malaysia

[#]Institute of Petroleum Engineering, Heriot-Watt University Malaysia, Precinct 2, 62100, Putrajaya, Federal Territory of Putrajaya, Malaysia

[§]Chemical Engineering Department, Universiti Teknologi PETRONAS, Bandar Seri Iskandar, 31750 Tronoh, Perak, Malaysia

[‡]Cairn India Ltd., Vipul Plaza, Sun City, Sector 54, Gurgaon 1222002, Haryana, India

ABSTRACT: This paper presents a significant finding where capillary-aided catastrophic gas hydrate growth is observed under a shut-in condition (static fluid) for an uninhibited system. With the use of a newly designed apparatus, consisting of six units of identical rocking cell, nucleation and growth are observed. All experiments are conducted under isochoric conditions using 11.0 K subcooling (ΔT_{sub}) as a driving force. A simulated natural gas mixture of 90.0 mol % methane + 10.0% mol % propane is used as a gas phase. The liquid phase used is 3% (Na^+, Cl^-) brine. The observations of the capillary-aided mass-transport mechanism for a catastrophic gas hydrate growth are presented in this work. Our observations show hydrate crystal formation at a brine wetted area close to the brine/gas interface initiates capillary-aided catastrophic hydrate growth. Moreover, no mass transfer restriction of brine toward catastrophic gas hydrate growth is observed. Furthermore, our results show the denser (less porous appearance) hydrate structures are continuously displaced from the hydrate−water interface (hydrate growth side). This displacement allowed new hydrate crystals to be formed uninterruptedly until the exhaustion of water in the cells. On the basis of macroscopic observations, the capillary-aided mass-transport mechanism for a catastrophic gas hydrate growth is presented.

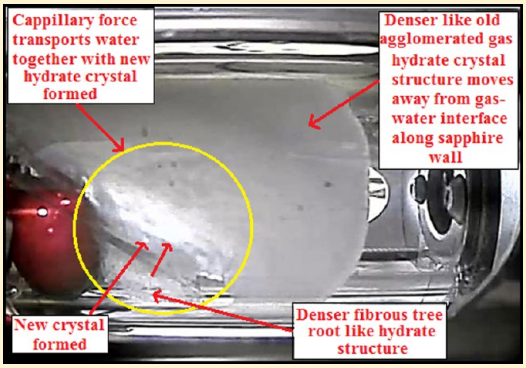

1. INTRODUCTION

Clathrate hydrates or gas hydrates are nonstoichiometric crystalline compounds that are formed in mixtures of water and nonpolar or slightly polar low molecular weight gases or volatile liquids when subjected to extreme conditions of high pressures and low temperatures.[1] There are three commonly studied gas hydrate structures that can be formed according to the guest molecule size: cubic structure I (sI), cubic structure II (sII) and hexagonal structure H (sH).[2−4] Recently, novel hydrate-related technologies have attracted attention in the energy and environmental fields. Some of these technologies are used in practical application such as energy transport and storage of gases, refrigeration and gas separation.[4] Moreover, natural gas deposits in the ocean permafrost, ocean trenches and continental margins is suggested to provide a possible energy source in the future.[2,5]

In the petroleum industry, formation of a gas hydrate in oil and gas transmission lines leads to catastrophic economic losses, pipeline blockages, and ecological risk as well as safety hazards.[3,6,7] The significance of preventing such losses due to pipeline blockages has initiated a new discipline of engineering known as flow assurance.[3] One of the main responsibilities of flow assurance engineering is to analyze risk associated with the presence of solids, such as gas hydrates. With advancing research and development over the past two decades, a more economical and environmental friendly hydrate risk management system using chemicals such as low-dosage hydrate inhibitors (LDHI) has emerged. The use of LDHIs (less than 1 wt % of water) is significantly cheaper and less hazardous compared to using the traditional hydrate prevention method with chemicals such as thermodynamic inhibitors (methanol or glycol) where the dosage can be as high as 60 wt % of water.[2] These LDHIs are designed either to delay hydrate formation (kinetic inhibitors) or to allow a controlled hydrate formation to occur in a dispersed flowing form (antiagglomerates).[2,3] Increasing demand of energy is challenging the petroleum industry to explore and produce oil and gas from more extreme environments with higher pressures and lower temperatures that fall far under the gas hydrate formation favorable conditions. Clearly, the advancement of the petroleum industry to produce from extreme environments is leaving more room for investigating the potential of gas hydrate formation risk under various production conditions.

To prevent or manage gas hydrate formation risks, the in-depth understanding of hydrate growth mechanism is important.[8−10] The general consensus is the formation of gas hydrate crystals alone will not guarantee a gas hydrate blockage

Received: November 5, 2014
Revised: January 5, 2015
Published: January 13, 2015

DOI: 10.1021/cg501626h
Cryst. Growth Des. 2015, 15, 1233−1241

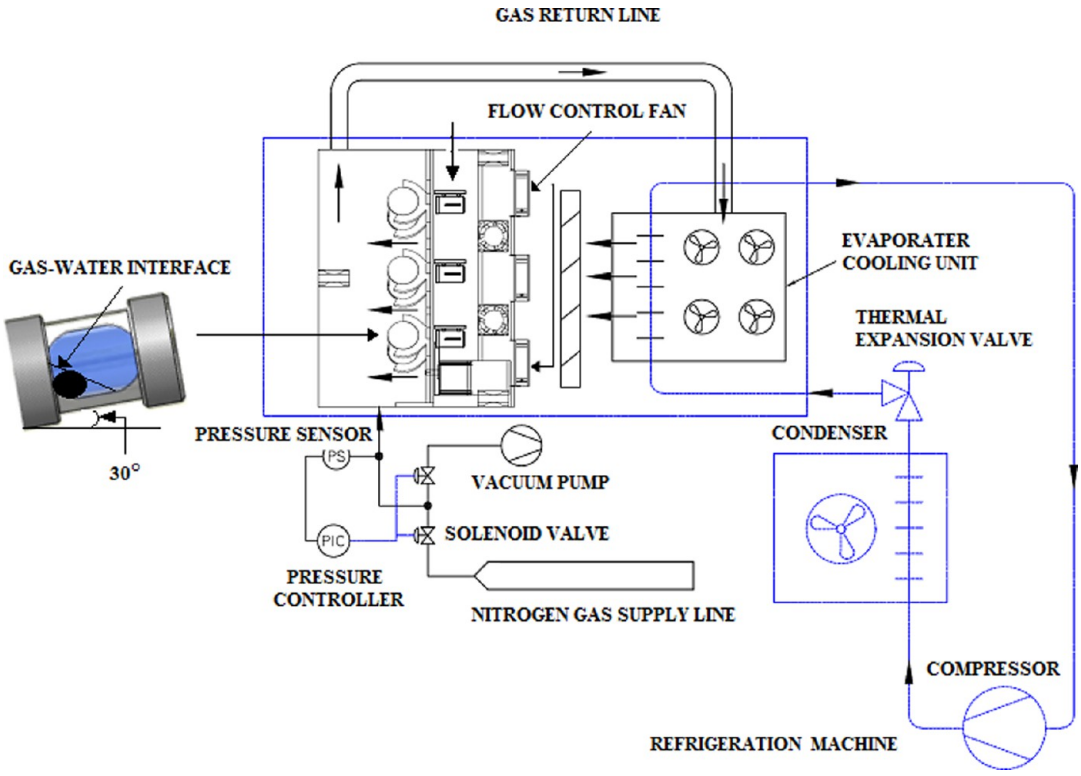

Figure 1. Schematic diagram of the experimental apparatus.

to occur in petroleum transmission lines.[2] The root cause identified for gas hydrate blockage in petroleum transmission lines is the gas hydrate crystals' ability to agglomerate while rapidly growing to a point where a cross-section of a pipeline is blocked. Therefore, hydrate growth kinetics is the main problem in hydrate risk management. Knowing the significance of gas hydrate growth kinetics to cause a blockage, in-depth understanding of hydrate kinetic mechanism is important. It has been pointed out that hydrate kinetics are governed by the transport mechanism of water and guest molecules toward a hydrate crystal.[11,12] Noyes and Whitney stated that a crystal surface such as a gas hydrate may provide a lower Gibbs energy that forms a boundary layer.[13] This boundary layer then supports crystal growth through diffusion of solutes toward a crystal growth.[13] Therefore, the crystal growth rate is determined by diffusion from the bulk concentration to the crystal interface. With extensive research done to evaluate this hypothesis, a breakthrough is made using interferometry experiments.[12−14] Researchers found physical evidence that shows the existence of a boundary layer at a growing surface to allow diffusion.[12−14]

The importance of a high concentration gradient to accelerate gas hydrate growth may be used to explain the tendency of hydrate to form first at interfaces between the water-rich phase and a guest molecule-rich phase, such as methane or CO_2.[10,15−17] However, once a layer of gas hydrate forms at the gas−water interface (static condition), further gas hydrate formation is reported to be retarded with no further growth.[11] A similar observation by other researchers leads to a suggestion that over a period of time, the hydrate layer growing at the gas−water interface may become less porous, which then slowly restricts mass transfer of water and guest molecules through the hydrate layer causing a hydrate growth to cease.[11,12,18,19] Breakthrough experimental work pioneered by Staykova[12] using FE-SEM imaging on gas hydrate structure found evidence that hydrate pores can transport water and gas. Therefore, this finding strengthens the hypothesis that if a hydrate pore becomes less permeable at the hydrate−water interface, mass-transport restriction will deplete the high concentration gradient of guest molecules necessary in bulk water to support further gas hydrate growth.[11,12,18,19]

The fundamental knowledge acquired from gas hydrate growth morphology is significant in industrial process optimization, where prediction of macroscopic flow or transport characteristics may be possible.[20,21] Among them, the discovery of different morphologies of hydrate crystals at the gas−water interface has been observed at different degrees of subcooling.[9,10,22] This observation has been noted for static[5,6,9,11] and also dynamic conditions.[19−21] Some reported morphological studies relevant to natural gas conditions also show that changes of hydrate structure are possible under different conditions.[10,22] However, to the best of our knowledge, the influence of different hydrate morphology found[9,10,22] on gas hydrate growth kinetics or mass transfer efficiencies is still not known. Moreover, findings on the simulated hydrate growth mechanism that may explain catastrophic gas hydrate growth under shut-in conditions (static) in natural gas pipelines could not be found from related literature.

This paper thus aims to report on the macroscopic observations made during a catastrophic gas hydrate growth for a simulated natural gas system under a shut-in condition (static). To mimic shut-in conditions, all the observations are carried out at a driving force of 11.0 K subcooling (ΔT_{sub}), which is similar to a gas transmission line that has been shut-in at seabed temperature (284.15 K). The chosen chemical composition and experimental parameter in this work are close to an actual deep-water gas production transmission line that has a previous history of gas hydrate formation. Lastly, the catastrophic growth mechanism in a simulated natural gas system is presented and described.

DOI: 10.1021/cg501626h
Cryst. Growth Des. 2015, 15, 1233−1241

2. EXPERIMENTAL APPARATUS AND PROCEDURES

Materials. A premix gas mixture of 90% molar methane and 10% molar propane with 98% purity from National Oxygen Pte Ltd. is used in this experiment. Sodium chloride with >99% purity for brine preparation was purchased from Sigma-Aldrich. Distilled and deionized water was used in throughout this experiment.

Apparatus. Figure 1 is the schematic of the experimental apparatus used for this present paper. The newly designed apparatus consists of six units of identical rocking cells. Each cell is made of durable sapphire glass to allow visibility for both the naked eye and also an online video camera to capture the reaction while working with high pressure up to 150 bar. Glass ball with a selected diameter is inserted in the cell to provide enhanced mixing of brine and gas before the experiment is started. A hard Teflon chemical resistant gasket is selected to seal the reactor ensuring no gas escaped from the high pressure reactor. Temperature measurements are made using a IMF Electronics RTD thermoprobe (TT0281) with an accuracy of ±0.15 K up to 160 bar. Pressure measurements are made with IMF Electronics pressure transducer (PT3541) with an accuracy of ±1.0% up to 400 bar. Total volume of the high pressure cell is 21.0 mL. Temperature control for this experiment is a custom designed air flow chamber for precise temperature control in cells and between cells. The environment control cabinet also holds a 6 high definition digital Moxa camera installed on the rear side of cell to have visual recording during experiments. A custom design rocking mechanism and ball count mechanism are also part of the temperature control chamber. The cells are mounted on a custom design rocking mechanism. All the functions and measurements are controlled by a programmable logic controller (PLC) integrated to tailored comprehensive software.

Experimental Procedures. Stringent cleaning work is applied for cell preparation and cell assembly, ensuring all wetting parts of the cell are ultra-clean. A vacuum is applied to remove impure air inside the cell. 10 mL of preweighted 3% brine is carefully injected into each cell, and the syringe is reweighted again. The 10.0 mL volume occupies 50% of the cell total volume. Premixed gas is pumped into the cells until a stable pressure of 40 ± 2% bar is achieved. The cells are then mounted on a custom design rocking mechanism. The environmental chamber is then vacuumed to remove moisture from air in the temperature control chamber before it is prefilled with dry nitrogen gas. Before a hydrate formation experiment for a shut-in condition starts, the cells are subjected to dynamic condition aided by the rocking mechanism and glass ball for 24 h. This is to allow good mixing between brine and premixed gas. After 24 h, rocking is stopped to simulate a shut-in condition. The cell composition is rapidly cooled at a rate of 0.24 K/min. This temperature gradient is similar to one of the selected subsea pipeline shut-in cooling gradients. The system is kept at ΔT_{sub} of 11.0 K (subcooling from sea-bed temperature) for 24 h for each experiment. By utilizing CSMGem,[11] it is determined only sII gas hydrates were formed in the experimental cells. Upon completion of the 24 h shut-in period at 11.0 K ΔT_{sub}, the cells are heated to 10.0 K higher than the hydrate dissociation temperature for a few hours. This is done to dissociate the gas hydrate formed in the cells. Experiments are then repeated for five cycles with two identical cells for each cycle. Upon completion of five cycles, a new batch of the same chemical composition is charged into the cell after cleaning the cell. The experiments are then repeated again five times for catastrophic hgas hydrate growth measurement. The subcooling here is the difference between sea-bed temperature (277.0 K) and our cells hydrate equilibrium temperature (288.0 K) determined by experimental work separate from this work. In all experiments, visual observation is made with the cell positioned at 30 degree inclinations. Thirty degree inclination is the standard position of the cell when the rocking mechanism is stopped. In this work, the cell composition consists of 10.0 mL of 3.0% wt NaCl with a gas pressure of 40 ± 2% bar of gas mixture.

3. RESULTS AND DISCUSSION

Catastrophic Hydrate Growth Initiation in the Vicinity of Water Surface. Figure 2 is the close-up macroscopic view presented in time intervals to illustrate a typical capillary force aided catastrophic growth mechanism found in this work. The detection of first gas hydrate structure in the bulk water is seen after 781 min exposed under an 11.0 K ΔT_{sub} condition (Figure 2a). The first gas hydrate structure has a fine tangled fibrous appearance. After 4 min (Figure 2b), the tangled hydrate fiber has slowly grown and branches to form a fibrous tree rootlike structure as shown in Figure 2c. Similar to this present work (Figure 2b,c), earlier morphological work by Lee[20] using a microscope confirms that a tangled fibrous dendrite-like gas hydrate structure will form in bulk water when the ΔT_{sub} >7.5 K. The formation of a fibrous gas hydrate structure at the water surface would be first thought to be a barrier for mass transfer. However, this was not the case observed from the experimental work. The fibrous structure did not evolve to form a diffusion barrier at the gas−water interface as shown in Figure 2c. Instead, the growing dense fibrous structure retained sufficient porosity for water mass transfer aided by capillary action toward the growing gas hydrate structure. Later in this experiment as shown in Figure 2d, a tiny water droplet (wetted surface) above the water−gas interphase forms a hydrate crystal. Upon formation of a hydrate crystal on the 860th minute, a communication (hydrate crystal) to the nearby water bulk which has the tangled fibrous dendrite gas hydrate structure occurs. The communication established between crystals adhered to sapphire glass and bulk water is the initiating point for a capillary transport for water (brine). As the hydrate formation continued on the sapphire glass surface, the water level started to decrease (Figure 2f−h). This indicates that a lot of water is necessary for gas hydrate growth. As the water level recedes, the tangled fibrous dendrite hydrate structures still remained and have a denser appearance. The fibrous tree root-like dendrite hydrate structures remained until the exhaustion of free brine (Figure 2h). The dense fibrous structure in the bulk water retained sufficient porosity for water mass transfer aided by capillary action toward the growing gas hydrate structure. Finally, the capillary-aided mass transfer leads to a catastrophic hydrate growth 887 min later (Figure 2h) after the detection of first gas hydrate structure. The phenomena of gas hydrate growth observed (Figure 2d−h) above the bulk water interface shows that gas hydrates have affinity to grow on sapphire glass. Furthermore, this observation on capillary action initiation (Figure 2d,e) is found to be similar to Henriksson's[23] work; initiation of a capillary force with surface energy differences between two phases. Henriksson[23] explained that a surface energy difference is created between water wet solid structure and bulk water under a close vicinity. The surface energy difference then creates a driving between a water wet solid and bulk water where a capillary action is innitiated[30] as observed in Figure 2d,e. Although Henriksson's[23] work is not related to gas hydrates, it can be used to explained the capillary action initiated when a water wet gas hydrate crystal[23,24] is formed in close vicinity to the bulk water as observed in this work (Figure 2d,e). Therefore, the surface energy difference between water wet solid (gas hydrate) and bulk water creates a driving force for capillary-aided crystal growth. Furthermore, by forming more gas hydrates, reduction of Gibbs free energy for a favorable equilibrium condition can be achieved.[11] Therefore, this may have further enhanced the initiated capillary action to carry on. As a result, a catastrophic gas hydrate growth covering a large section of a sapphire glass occurred as observed in this paper (Figure 2h).

Since the capillary-aided catastrophic gas hydrate growth mechanism extends beyond the area of gas−water interface, time interval macroscopic observation covering the entire cell sapphire interior is also conducted. The following sections in this

DOI: 10.1021/cg501626h
Cryst. Growth Des. 2015, 15, 1233−1241

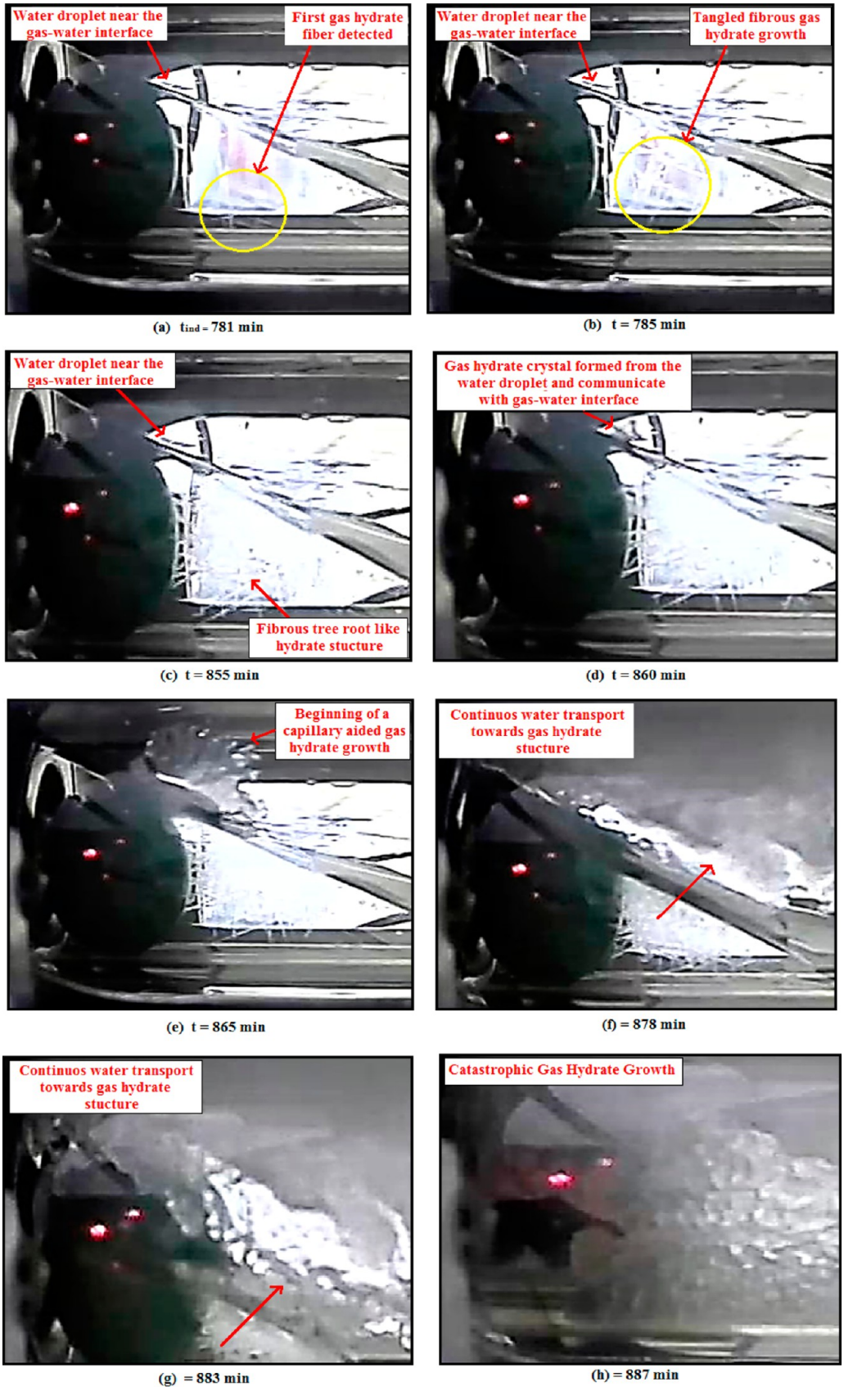

Figure 2. Close-up view of a typical catastrophic growth mechanism.

paper will illustrate macroscopic observation of four separate cases where a capillary-aided catastrophic gas hydrate growth is found in the vicinity of (a) gas−water interface, sapphire glass, and glass ball, (b) gas−water interface, sapphire, glass ball, and

DOI: 10.1021/cg501626h
Cryst. Growth Des. 2015, 15, 1233−1241

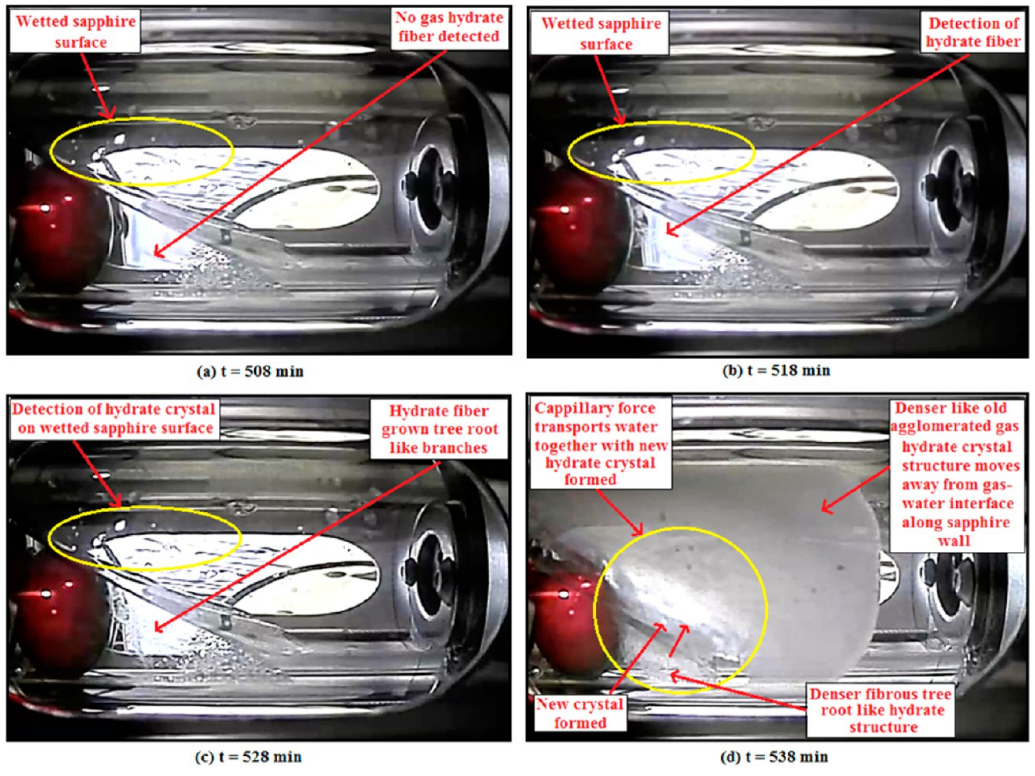

Figure 3. Sequential images of gas hydrate growth under subsea conditions with a ΔT_{sub} of 11.0 K.

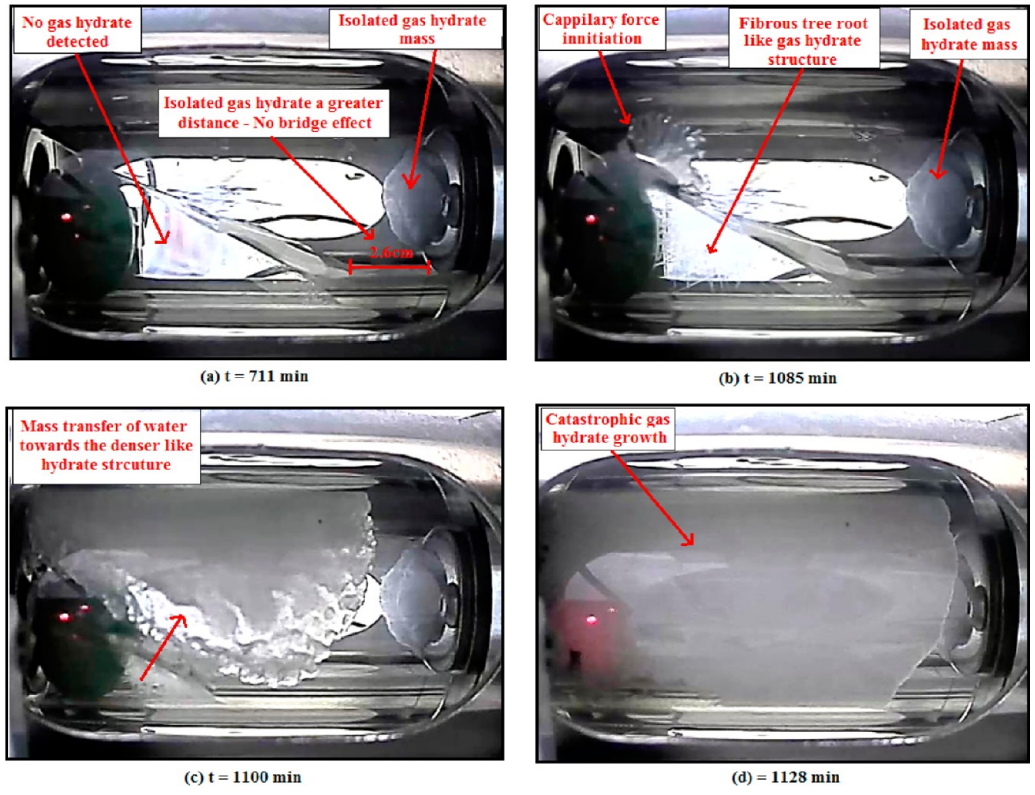

Figure 4. Catastrophic gas hydrate growth with an efficient mass transfer.

isolated gas hydrate structure, (c) gas−water interface, sapphire, and isolated gas hydrate structure, and (d) gas−water interface, sapphire, glass ball, and metal surface. Close up macroscopic images in Figure 2 is revisited during image presentation and discussion of the four separate cases presented in this paper.

Case 1: Catastrophic Gas Hydrate Growth in the Vicinity of Water Surface (Gas−Water Interface, Sapphire Glass, and Glass Ball). In Figure 3, a catastrophic gas hydrate growth is presented in 10 min intervals. No gas hydrates are detected in the cell after 508 min under a driving force of 11.0 K

DOI: 10.1021/cg501626h
Cryst. Growth Des. 2015, 15, 1233−1241

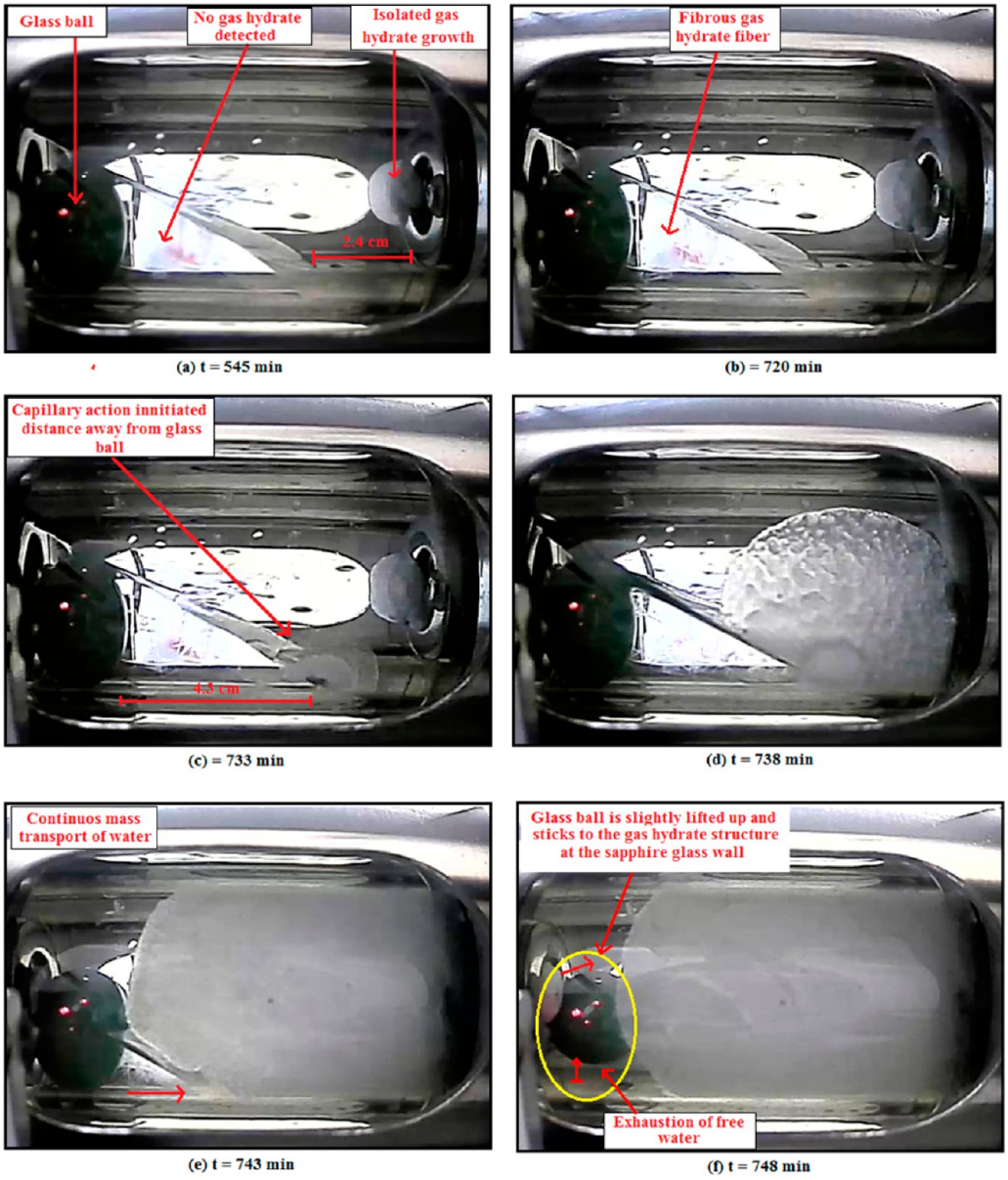

Figure 5. Initiation of capillary action away from glass ball for catastrophic gas hydrate growth.

ΔT_{sub}. However, 10 min later in Figure 3b, the first hydrate structures are detected. Similar to the close-up picture in Figure 2a, this hydrate structure (Figure 3b) has a fine tangled fibrous appearance in the bulk phase. After 10 min (Figure 3b), the tangled hydrate fibers have slowly grown and branch to form a fibrous tree root-like structure, but with no massive growth initiated. As soon as the wetted surface on the sapphire glass above the gas−water interphases near to the glass ball forms hydrate crystal on the 538th minute (Figure 3c) similar to Figure 2d; massive hydrate formation is initiated as shown in Figure 3d. Massive growth is continued with efficient water transport upward (Figure 3d) from a liquid bulk toward the growing crystal which had adhered to the sapphire glass. Similar to Figure 2d−g, the dense fibrous hydrate structure in the bulk water (Figure 3c,d) retained its porosity and did not stop the mass transfer of water toward the growing hydrate structure. During hydrate growth (Figure 3d), new hydrate crystals are observed to form near the gas−water interface. Interestingly, with a capillary-aided mass transfer, a unique gas hydrate crystal growth mechanism is observed. The newly forming hydrate crystal near the bulk water is seen to push or displace the existing (older) crystals away from its birthplace (gas−water interface). The older hydrate crystal agglomerates along the sapphire wall and are denser in appearance as shown during the 548th minute (Figure 3d). As a result, continued access of gas to the water surface which provided the materials essential for further crystal grow[10,11,25] is possible under this unique crystal growth mechanism. Therefore, mass transfer restriction that retards further hydrate growth due to porosity reduction at the gas−water interface[10,11,16,24,26] is prevented with this unique gas hydrate growth as shown in Figure 3d.

Case 2: Catastrophic Gas Hydrate Growth in the Vicinity of Water Surface (Gas−Water Interface, Sapphire, Glass Ball, and Isolated Gas Hydrate Structure). Figure 4 is sequential images of a capillary-aided catastrophic gas hydrate growth that occurred without being triggered by an isolated mass of gas hydrate formed within the same experimental cell. A patch of hydrate mass is seen to form at a distance

DOI: 10.1021/cg501626h
Cryst. Growth Des. 2015, 15, 1233−1241

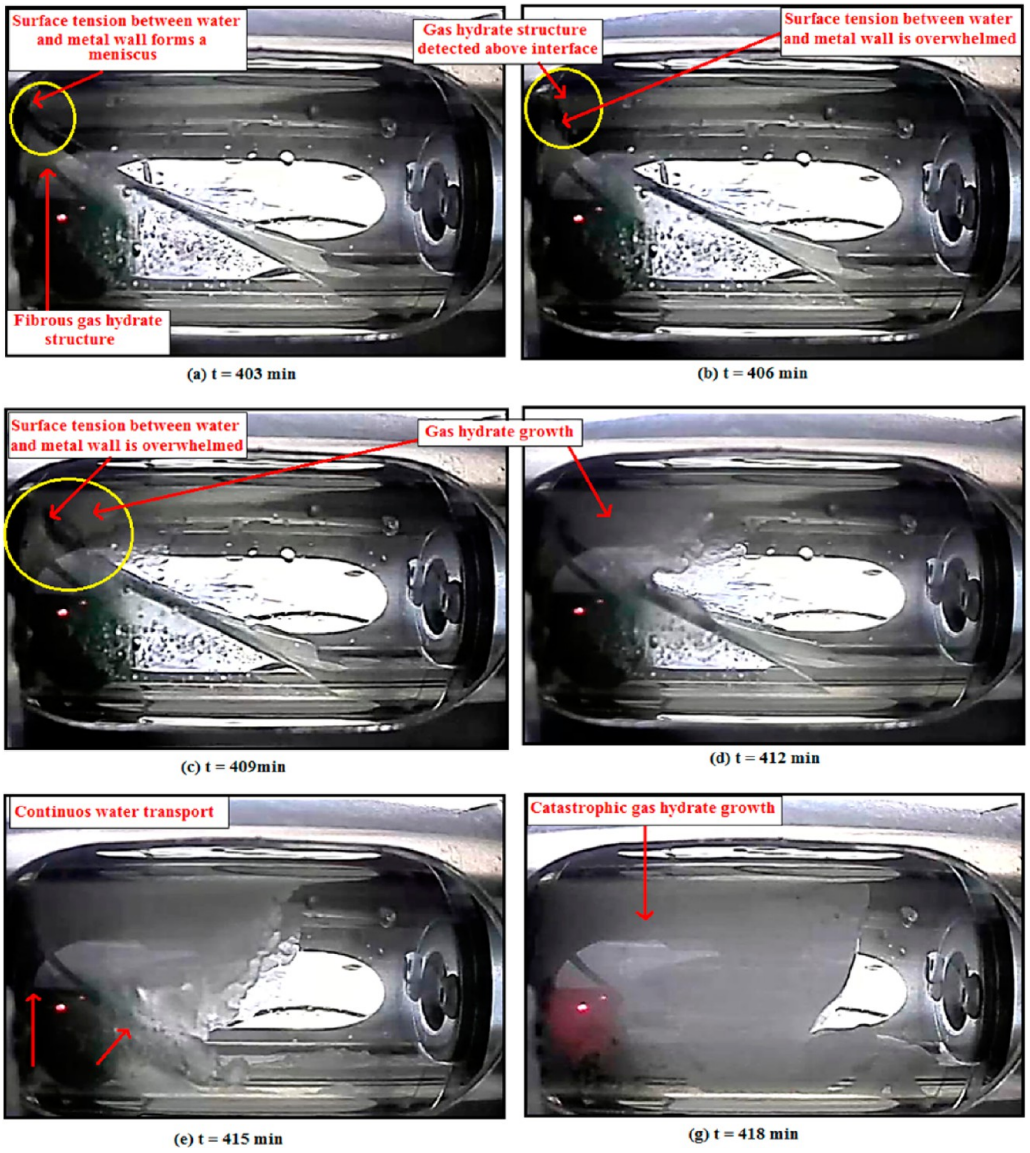

Figure 6. Surface tension disturbance during initiation of capillary action for catastrophic.

(2.6 cm) from bulk water as illustrated in Figure 4a. This is after 711 min under ΔT_{sub} of 11.0 K. There is no communication or any sort of reported bridge effect[27,28] between the bulk water and the isolated hydrate mass to trigger any gas hydrate growth in the liquid bulk. Similar to Figures 2d and 3c, when a gas hydrate crystal forms near the liquid interphase with the presence of a fibrous tree root-like structure in the bulk water, a capillary-aided gas hydrate growth is initiated 375 min later (Figure 4b). Figure 4c shows the repetition of observations made in Figure 3d where a unique growth mechanism is seen pushing the existing agglomerated crystals away from the interface along the sapphire surface, while the mass transfer of water through the porous fibrous hydrate structure in the bulk water was continued. After 1128 min (Figure 4d), a catastrophic gas hydrate growth is noted.

Case 3: Catastrophic Gas Hydrate Growth in the Vicinity of Water Surface (Gas–Water Interface, Sapphire, and Isolated Gas Hydrate Structure). Figure 5 shows the sequential images of a capillary-aided catastrophic gas hydrate growth occurring 4.3 cm away from the glass ball. Similar to Figure 4, isolated gas hydrate formed at a greater distance (2.4 cm) in Figure 5a did not initiate a gas hydrate growth immediately in the bulk water. However, 175 min later (Figure 5b), a fibrous gas hydrate structure is detected in the liquid bulk. This time, a capillary-aided gas hydrate growth is initiated at a wetted surface above a gas–water interface at a greater distance (4.3 cm) from the glass ball (Figure 5c). Upon catastrophic gas hydrate growth 15 min later (Figure 5f), the glass ball is observed to be slightly lifted upward and sticking to the sapphire glass wall opposite of the camera view. Mass transport until the point of free brine solution being exhausted similar to Figures 2–4 is observed (Figure 5e,f). Moreover, even the last free brine located in a 30 degree gradient below the hydrate mass is transported to the hydrate mass until the free brine is exhausted through the porous fibrous hydrate structure in the bulk water (Figure 5e,f). Even though the initial chemical composition of the water before hydrate formation contains only 3% brine (Na^+ and Cl^-), ions such as Na^+ and Cl^- are known to be excluded from gas hydrate clathrates structures during growth.[11,24,29,30] Therefore, with increasing brine concentration due to ion exclusion during gas hydrate growth, the thermodynamic inhibition property of the brine would also increase.[11,23,28,29] If the driving force is insufficient with the

DOI: 10.1021/cg501626h
Cryst. Growth Des. 2015, 15, 1233–1241

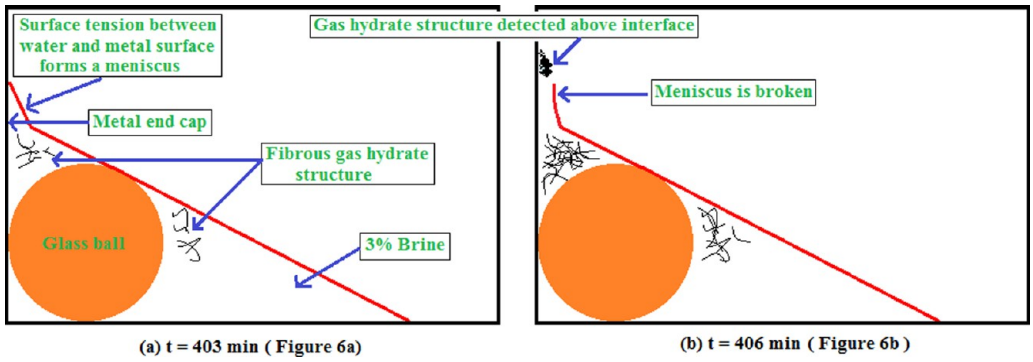

Figure 7. Pictorial images of (a) Figure 6a and (b) Figure 6b for visual clarity.

increasing thermodynamic inhibition property of brine during hydrate growth, further gas hydrate formation is expected to be retarded at a certain stage.[24,30] However, in this work, the capillary-aided water transport observed continued until all free water is exhausted (Figure 5f).

Case 4: Catastrophic Gas Hydrate Growth in the Vicinity of Water Surface (Gas−Water Interface, Sapphire, Glass Ball, and Metal Surface). Figure 6 presents a capillary-aided catastrophic gas hydrate growth which started at the metal wall (end-cap of the cell) just above the gas−water interface in a 3 min time interval. In Figure 6a, a meniscus is formed due to surface tension between water bulk and the metal wall. Despite the presence of a fibrous gas hydrate structure below the water−gas interface, the meniscus remained undisturbed (Figure 6a).

However, when a gas hydrate crystal is detected slightly above the interface, the meniscus between gas−water interfaces (Figure 6b) is broken. This is followed by an efficient water transport through the porous fibrous hydrate structure in the bulk water (Figure 6c−e) toward the growing gas hydrate growth structure. The free brine is then exhausted while a catastrophic gas hydrate growth is observed (Figure 6f). Similar to this observation (Figure 6), researchers[31,32] also found and explained similar capillary action initiation in the area of hydrodynamics. Levich[31] and Sphhocleous[32] explained that any disturbance in surface tension may cause a meniscus to break leading toward a capillary action. The formation of water wet gas hydrate crystal in Figure 6b (similar to the close-up image in Figure 2d) slightly above the meniscus, caused the meniscus to break and a capillary action to be initiated. The capillary-aided mass transfer initiated after breaking the meniscus resulted in a catastrophic gas hydrate growth 12 min later (Figure 6g). Figure 7 is a pictorial illustration presented to provide better visual clarity of Figure 6a,b.

4. CONCLUSIONS

The capillary-aided catastrophic hydrate growth where a whole pipe cross section blocked due to hydrate formation under a shut-in condition is observed in the present work. Experiments were conducted under a driving force of 11.0 K ΔT_{sub} with a simulated natural gas mixture of 90.0 mol % methane + 10.0% mol % propane at pressure of 40 ± 2% bar. The novel aspect of this work is in how physical factors come into play in accelerating growth beyond what would be expected from diffusion kinetics in the water phase. Thus, these observations of capillary-aided hydrate growth expand knowledge of the kinetics of crystal growth through detailed observation of the growth process. The results can be summarized as follows: (1) Hydrate crystal formation at a brine-wetted area close to the brine/gas interface initiates capillary-aided catastrophic hydrate growth. This region of hydrate crystal formation has fast transport of gas molecules and rapid water transport through reduction in surface tension and capillary effect under a shut-in condition. Furthermore, the capillary action causes a large increase in water surface area for gas diffusion over a short range and maintains the supply of water to the growing crystals. (2) Hydrate formation retardation due to increasing concentration of brine (Na^+ and Cl^-) is not observed. Hydrate growth continued until all the visually seen water is exhausted. (3) The ability of new hydrate crystal growth pushing the denser old formed hydrate crystal due to agglomeration away from the growth zone does not allow decreasing porosity on a dense hydrate mass as a growth limiting factor. This mechanism allows continues water transport to the growing hydrate structure via a capillary effect until the exhaustion of the water. (4) On the basis of morphology observations, the mechanism of a capillary-aided catastrophic gas hydrate growth is presented.

AUTHOR INFORMATION

Corresponding Author

*Phone: +603 88810918. Fax: +60388810194. E-mail: k.msabil@hw.ac.uk.

Notes

The authors declare no competing financial interest.

ACKNOWLEDGMENTS

The authors are grateful to Baker Hughes (M) Sdn. Bhd and Universiti Teknologi PETRONAS for providing financial support and facilities. The authors would also like to thank Dixson FA Engineering for their technical skills of fabrication of rocking cell and support. Thanks also to Richard Bremer (ICSS/DCS) and Yeah Swee Lin (SCADA) for their contribution in this work.

REFERENCES

(1) Ishida, Y.; Sakemoto, R.; Ohmura, R. *Chem.—Eur. J.* **2011**, *17*, 9471−9477.
(2) Koh, C. A. *Chem. Soc. Rev.* **2001**, *31*, 157−167.
(3) Sloan, E. D. *Nature.* **2003**, *426*, 353.
(4) Seo, Y.; Kang, S. P. *J. Petrol. Sci. Eng.* **2012**, *88−89*, 61−66.
(5) Anderson, R.; Llamendo, M.; Tohidi, B.; Burgass, R. W. *J. Phys. Chem. B* **2003**, *107*, 3507−3514.
(6) Ohno, H.; Susilo, R.; Gordienko, R.; Ripmeester, J.; Walker, V. K. *Chem.—Eur. J.* **2010**, *16*, 10409−10417.
(7) Davies, S. R.; Sloan, E. D.; Sum, A. K.; Koh, C. A. *J. .Phys. Chem. C* **2010**, *114*, 1173−1180.
(8) Kashchiev, D.; Firoozabadi, A. *J. Cryst. Growth.* **2003**, *250* (3−4), 499−515.

DOI: 10.1021/cg501626h
Cryst. Growth Des. 2015, 15, 1233−1241

(9) Bruusgaard, H.; Lessard, D. L.; Servio, P. *Cryst. Growth Des.* **2009**, *9*, 3014−3023.
(10) Watanabe, S.; Saito, K.; Ohmura, R. *Cryst. Growth Des.* **2011**, *11*, 3235−3242.
(11) Sloan, E. D. *Clathrate Hydrates of Natural Gases*, 2nd ed.; Marcel Dekker: New York, 1998.
(12) Staykova, D. K.; Kuhs, W. F.; Salamatin, A. N.; Hansen, T. *J. Phys. Chem. B* **2003**, *107*, 10299−10311.
(13) Noyes, A. A.; Whitney, W. R. *J. Am. Chem. Soc.* **1897**, *19*, 930−934.
(14) Bunn, C. W. *Discussion Faraday Soc.* **1949**, *5*, 132.
(15) Davies, S. R.; Sloan, E. D.; Sum, A. K.; Koh, C. A. *J. Phys. Chem. C* **2010**, *114*, 1173−1180.
(16) Kumar, R.; Lee, J. D.; Song, M.; Englezos, P. *J. Cryst. Growth* **2008**, *310*, 1154−1166.
(17) Takeya, S.; Hori, A.; Uchida, T. *J. Phys. Chem. B* **2000**, *104*, 4164−4168.
(18) Fandino, M.; Ruffina, L. *Fuel.* **2014**, *117*, 442−449.
(19) Zhong, D. L.; Yang, C.; Liu, D. P.; Wu, Z. M. *J. Cryst. Growth* **2011**, *327* (1), 237−244.
(20) Lee, J. D.; Song, M.; Susilo, R.; Englezos. *Cryst. Growth Des.* **2006**, *6* (6), 1428−1439.
(21) Lim, Y. A.; Baby, P.; Kumar, R.; Lingga, P. *Cryst. Growth Des.* **2013**, *13*, 2047−2059.
(22) Saito, K.; Kishimoto, M.; Tanaka, R.; Ohmura, R. *Cryst. Growth Des.* **2011**, *11* (1), 295−301.
(23) Henriksson, U.; Ericksson, J. C. *J. Chem. Educ.* **2004**, *81*, 150−154.
(24) Sharifi, H.; Ripmeester, J.; Walker, V. K.; Englezos, P. *Fuel* **2014**, *117*, 109−117.
(25) Berg, W. F. *Proc. R. Soc. (London)* **1938**, *79*, A164.
(26) Lee, J. D.; Englezos, P. *Chem. Eng. Sci.* **2006**, *61*, 1368−1376.
(27) Servio, P.; Englezos, P. *AIChE J.* **2003**, *49*, 269−276.
(28) Lee, J. D.; Susilo, R.; Englezos, P. *Chem. Eng. Sci.* **2005**, *60*, 4203−4212.
(29) Jung, J. W.; Santamarina, J. C. *J. Cryst. Growth* **2012**, *345*, 61−68.
(30) Daraboina, N.; Malmos, C.; Solms, N. V. *Fuel* **2013**, *108*, 749−757.
(31) Levich, V. G.; Krylov, V. S. *Annu. Rev. Fluid Mech.* **1969**, *1*, 293−316.
(32) Sphhocleous, M. *Hydrogeol. J.* **2010**, *18*, 811−821.

DOI: 10.1021/cg501626h
Cryst. Growth Des. 2015, 15, 1233−1241